

2019 Rock Dynamics Summit– Aydan et al. (eds)  
© 2019 Taylor & Francis Group, London, ISBN 978-0-367-34783-3

## Study on dynamic shear strength and deformation characteristics of rock discontinuity

J. Yoshida & T. Sasaki  
*SUNCOH Consultant Co. Ltd., Tokyo, Japan*

R. Yoshinaka  
*Saitama University, Saitama, Japan*

**ABSTRACT:** The authors have developed a new dynamic direct shear test machine, for the purpose of investigating the response to the earthquake motion of rock discontinuities. We conducted a large number of dynamic direct shear tests for the rock discontinuities. Test specimens are Limestone joint, Sandstone joint and Mudstone bedding plane of natural discontinuity made by boring-core, and artificial discontinuities made of mortar. By these test results, we examined dynamic shear strength and dynamic shear deformability of rock discontinuity.

The authors defined dynamic peak shear strength  $\tau_{p(d)}$  by the results of Multi-stage amplitude dynamic direct shear tests. Then, we investigated comparison of dynamic shear strength and static shear strength, and dependence on frequency for dynamic shear strength. It is clear that dynamic shear strength exceeds static shear strength for relatively rough planes, and dynamic peak shear strength  $\tau_{p(d)}$  does not depend on the frequency in the range from 0.1Hz to 3.0Hz

Also we defined the dynamic diagonal shear stiffness  $K_{sd(d)}$  and attenuation  $h$ . Furthermore, we examine the stress dependence and frequency dependence of these dynamic deformability parameters. We defined skelton curves and modelled it by hyperbolic function. It is Clear that both the dynamic diagonal shear stiffness  $K_{sd(d)}$  and attenuation  $h$ , have a dependance about normal stress  $\sigma_n$  and shear stress amplitude.

### 1 GENERAL INTRODUCTION

Many rock discontinuities are distributed in hard rock such as bedding planes or joint planes, and influence the strength and deformability of the rock mass. In recent years, dynamic analysis method for rock foundations such as for very important facilities and on large rock slopes was required. With regard to this dynamic analytical method for discontinuous rock mass, the problems due to the conventional elastic analysis methods being insufficient are pointed out, but a new analytical method for rock foundation and rock structure has been proposed in recent years (Iwata et al., 2012; Yoshinaka et al., 2012).

However, in analysis and design using these analytical methods, dynamic strength and deformability of the rock discontinuity become the input parameters for analysis of the problem. Not much data has been accumulated on dynamic strength and deformability of rock discontinuities in the past, unlike that for the static parameters from laboratory core tests or in-situ tests. Furthermore, exclusive test machines are not generally available. Particularly, regarding dynamic cyclic load test machines for investigating the rock discontinuities that are assumed to occur in an earthquake, there are only a few research papers. But, among these

research papers, dynamic testing under the condition of assumed real seismic motions is almost non-existent.

The authors developed the new dynamic direct shear test machine which Figure 1 showed for the purpose of investigating the dynamic properties of rock discontinuity at the time of the earthquake (Yoshida et al., 2014). In this study, we examined the dynamic shear strength of rock discontinuity and dynamic shear properties than the test result using this test machine.

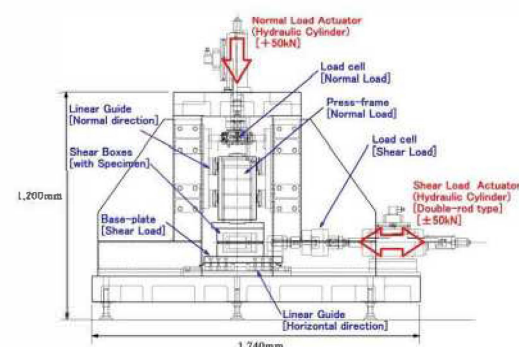


Figure 1. Dynamic direct shear test machine for rock discontinuity

## 2 DYNAMIC SHEAR STRENGTH OF ROCK DISCONTINUITY

### 2.1 Definition of dynamic shear strength

Figure 2 shows the result of Multi-stage amplitude dynamic direct shear test for limestone joints. The limestone joints in the tests were rough plane (JRC = 10~16 for observation) and were interlocking well (rank B). The frequency of the shear stress wave was 1.0 Hz, the shear stress amplitude arrived at the targeted strength (static shear strength,  $\tau_s$ ) after loading with 10 stages and 5 cycles of waves. Figure 2(b) shows the time history waveform of shear displacement, and Figure 2(c) shows the shear hysteresis.

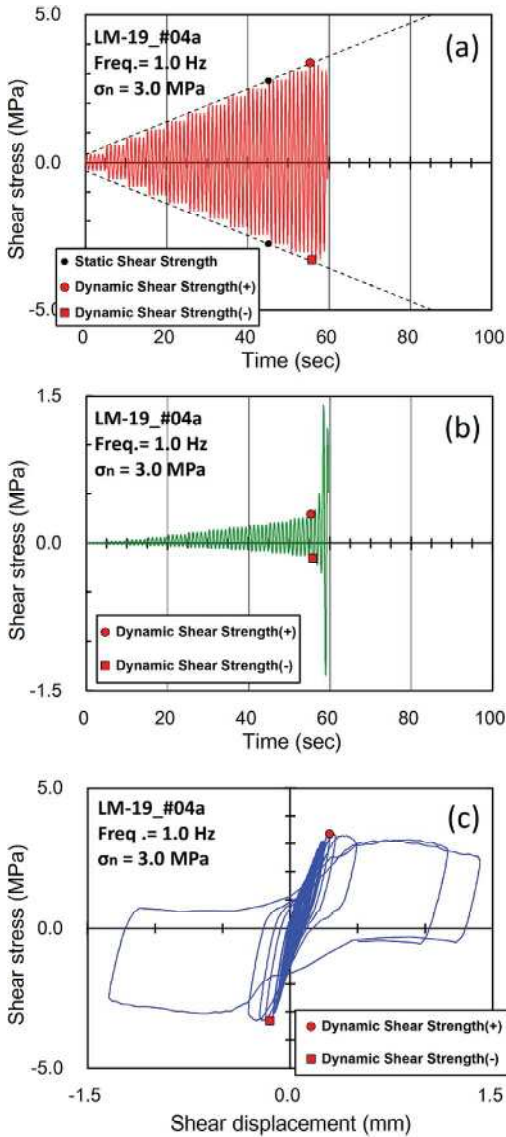


Figure 2. Result of Multi-stage amplitude dynamic direct shear test (Limestone joint, JRC=10~16)

Multi-stage amplitude dynamic direct shear test is performed by loading with M stages of N cycles of sine waves in succession, under a constant normal stress. After loading 10 stages with 5 cycles of sine waves, we planned that shear stress amplitude would reach the targeted strength. We set the target strength as the static shear strength,  $\tau_s$  of the same discontinuity. So, set the shear stress amplitude of the first stage to  $S=0.1\tau_s$ . Thereafter, the shear stress amplitude was increased stepwise:  $0.2\tau_s, 0.3\tau_s, 0.4\tau_s, 0.5\tau_s, \dots$ . In reality, the number of loading stages may exceed 10, because shear stress loading is continued until dynamic shear failure.

Figure 3 shows the time history waveform of the stress ratio  $R_s$ , which calculated about a shear stress amplitude wave both positive side and negative side. Stress ratio  $R_s$  is the ratio of peak value  $\tau_{pi}$  and target shear stress amplitude  $\tau_o$  every loading wave pattern 1 cycle, and it is calculated by the next expression.

$$R_s = \tau_{pi} / \tau_o$$

According to Figures 2 and 3, the shear stress gradually than 12<sup>th</sup>-stage of 3<sup>rd</sup>-wave decreases in an positive side, and the stress ratio,  $R_s$  is less than 0.95 in 12<sup>th</sup>-stage of 4<sup>th</sup>-wave. In negative side, the stress ratio,  $R_s$  is less than 0.95 in 12<sup>th</sup>-stage of 4<sup>th</sup>-wave equally. Similarly, the shear displacement suddenly increases in 12<sup>th</sup>-stage of 4<sup>th</sup>-wave in both sides of the positive and negative sides.

We define the dynamic peak shear strength,  $\tau_{p(d)}$  as follows.

When shear stress decreases continually after shear stress is less than 95% of target shear stress amplitude  $\tau_o$ , or when shear displacement exceeds 1.0mm, we define shear failure.

Dynamic peak shear strength  $\tau_{p(d)}$  is defined the maximum value of the shear stress amplitude before dynamic shear failure. In addition, dynamic peak shear strength  $\tau_{p(d)}$  is defines in both sides of positive and negative.

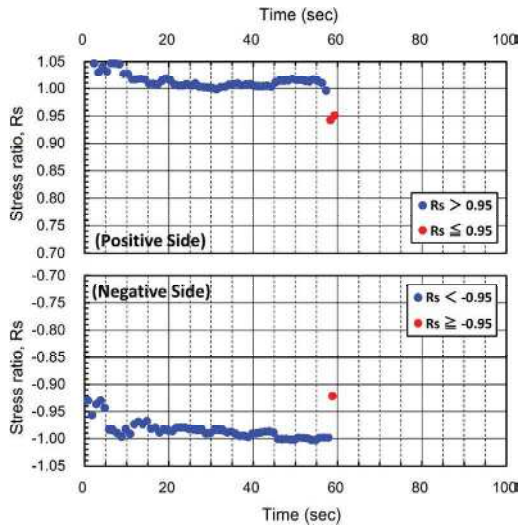


Figure 3. Stress ratio of positive and Negative sides

Figure 4 shows the failure envelope curve of the Multi-stage amplitude dynamic direct shear test result for a mortar tension crack (JRC = 8-12, interlocking = rank A). The mark of  $\circ$  and  $\square$  in Figure 4 are dynamic peak shear strength  $\tau_{p(d)}$  by an positive side and negative side. Solid line is Mohr-Coulomb's criteria which modelled these results, and the dashed line is an envelope curve of the static shear strength in a similar discontinuity. According to this, the shear strength of rock discontinuity understands that a dynamic strength exceeds static strength.

Figure 5 shows the test result of the case which assumed the frequency of the loading wave pattern 0.1Hz, 1.0Hz and 3.0Hz. According to this, the loading frequency dependence in dynamic peak shear strength  $\tau_{p(d)}$  is not recognized.

Figure 6 shows the result that modelled by Barton's criteria. Basic friction is  $\phi_b = 31.6^\circ$  is provided from ultimate shear strength by static shear tests. According to this, in JRC, dynamic strength (JRC = 24.1) exceeds static strength (JRC = 18.7).

Figure 7 shows the failure envelope curve which made from the results of Multi-stage amplitude dynamic direct shear tests for Limestone joints and Mud-stone bedding planes. This failure envelope curves are modeled in Mohr-Coulomb's criteria. Limestone joint is relatively rough (JRC=10~16 by observation), and the interlocking is slightly good (rank B). Mud-stone bedding plane is relatively flat (JRC=4~8 by observation), and the interlocking is slightly bad (rank C). Differences between dynamic

strength and static strength are big with the relatively surface rough Limestone joints, but, as for the difference, are not almost admitted in the relatively flat Mud-stone bedding planes.

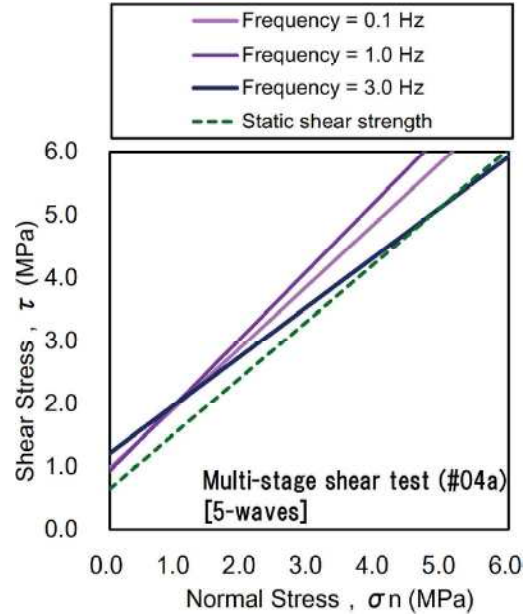


Figure 5. Frequency-dependent of dynamic strength (Mortar tension crack, JRC=8~12)

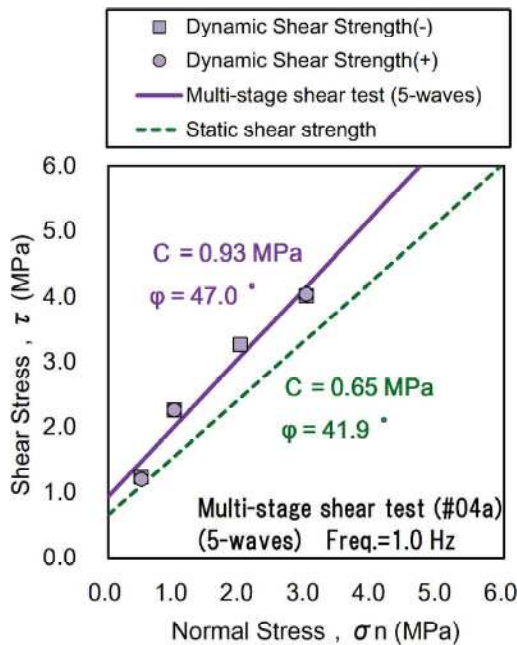


Figure 4. Failure envelope curve for dynamic strength and static strength (Mortar tension crack, JRC=8~12)

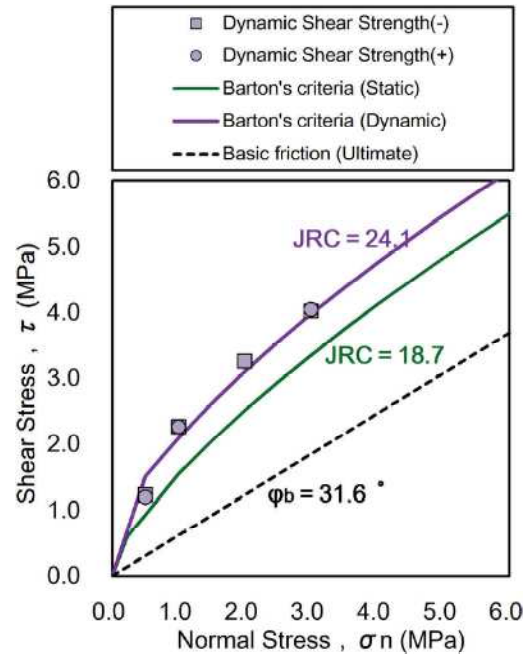
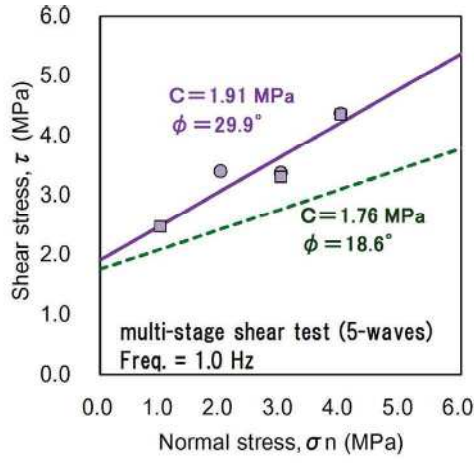
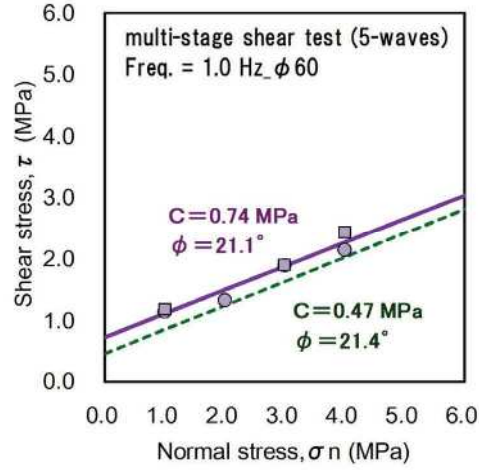


Figure 6. Barton's criteria (Mortar tension crack, JRC=8~12)



(a) Limestone joints (JRC=10~16, rank B)



(b) Mudstone bedding plane (JRC=4~8, rank C)

Figure 7. Dynamic shear strength of many type of rocks

### 3 DYNAMIC SHEAR DEFORMABILITY OF ROCK DISCONTINUITY

Like shear strength, Figure 8 shows the results of the Multi-stage amplitude dynamic direct shear tests for Limestone joints. Figure 8 showed the fifth wave shear hysteresis and dilation curve of each loading stage individually. According to this, loading almost presents a rectilinear figure to the sixth phase (0.6τs) from the first, but presents fusiform hysteresis afterwards. Large displacement and a drop of the shear stress are accepted to the 12<sup>th</sup>-stage (1.2τs) afterwards at both sides of the positive and negative. Such tendency was similar to the dynamic heteromorphic characteristic in the core test specimen.

We define dynamic shear parameters to investigate dynamic shear properties. Figure 9 shows a definition of dynamic diagonal shear stiffness,  $K_{sd(d)}$ .

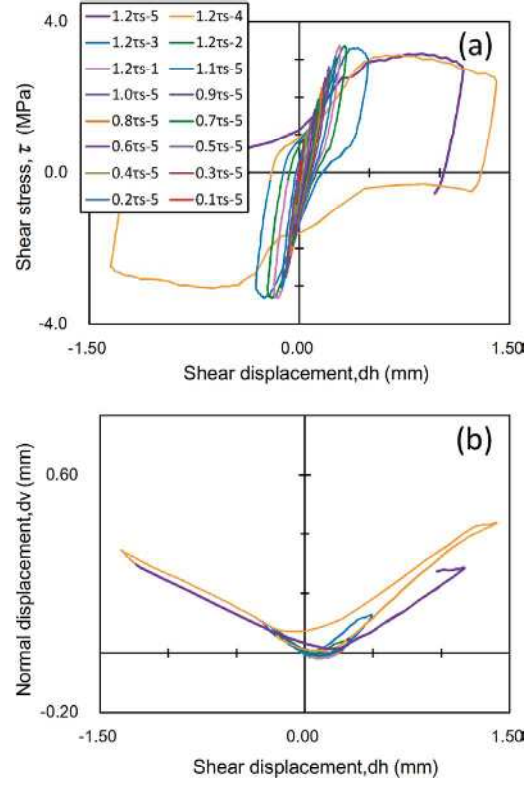


Figure 8. State of the deformation every loading stage (Limestone joint, JRC=10~16)

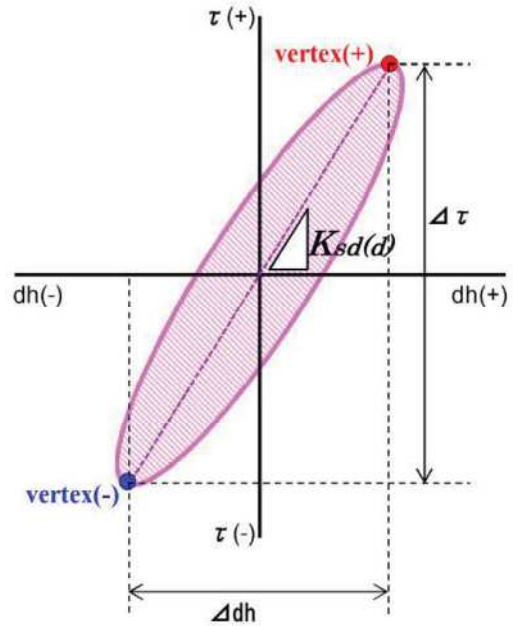


Figure 9. Dynamic diagonal shear stiffness,  $K_{sd(d)}$



We define dynamic diagonal shear stiffness  $K_{sd(d)}$  it with a straight line to link positive vertex and negative vertex of the shear in a Figure 9.

Dynamic diagonal shear stiffness,  $K_{sd(d)}$  is a shear stiffness to define about individual shear hysteresis, and is defined next expression.

$$K_{sd(d)} = \frac{\Delta\tau}{\Delta dh} \quad (\text{MPa/mm}) \quad (1)$$

where  $\Delta\tau$ : shear stress amplitude both sides (MPa)  
 $\Delta dh$ : shear displacement amplitude both sides (mm)

We define attenuation  $h$  by the next expression, as decrement energy in area  $\Delta W$  surrounded by shear hysteresis.

$$h = \frac{1}{2\pi} \frac{\Delta W}{W} \times 100(\%) \quad (2)$$

Equivalent elastic energy  $W$  is defined by the next expression.

$$W = \frac{1}{4} \Delta\tau \cdot \Delta dh \quad (3)$$

Figure 10 shows the example which calculated a dynamic shear parameter. We define dynamic diagonal shear stiffness,  $K_{sd(d)}$  with the incline of the straight line to link an equilateral positive vertex of the shear hysteresis and the negative vertex to show in Figure 9. In addition, attenuation,  $h$  is provided by calculating the area of the loop of the closed shear hysteresis.

Figure 11 plots it about a change for shear displacement both amplitude  $\Delta dh$  of dynamic diagonal shear stiffness,  $K_{sd(d)}$  and attenuation,  $h$  provided from Multi-stage amplitude dynamic direct shear tests result for Limestone joints. According to this, it is identified as both parameters to depend about

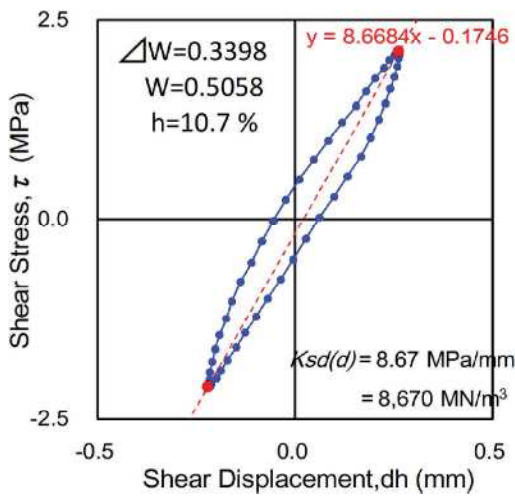


Figure 10. Example of dynamic shear parameters

the shear displacement amplitude namely the shear stress amplitude.

According to Figure 11(a), dynamic diagonal shear stiffness,  $K_{sd(d)}$  tends to decrease with increase in shear displacement both amplitude  $\Delta dh$  (i.e., shear stress both amplitude  $\Delta\tau$ ). Furthermore, a tendency to increase with increase in normal stress has it, and this tendency is common in the static shear.

Figure 11(b) plots it about a change for shear displacement both amplitude  $\Delta dh$  of attenuation,  $h$  provided than the same test result. Although a tendency to increase with increase in shear displacement both amplitude  $\Delta dh$  is seen, according to this, attenuation,  $h$  presents some decrease halfway. These causes include the thing with the reversely sigmoid model shear hysteresis by increase in shear displacement (i.e., the shear stress amplitude) as having been seen in a change of the shear hysteresis that mentioned above.

Figure 12 shows the shear hysteresis of the Multi-stage amplitude dynamic direct shear tests for mortar tension crack. Figure 12(a) is the figures which plotted positive vertex and negative top in the 5<sup>th</sup>-wave shear hysteresis every stage of the shear stress amplitude. The curve expressed by the set of

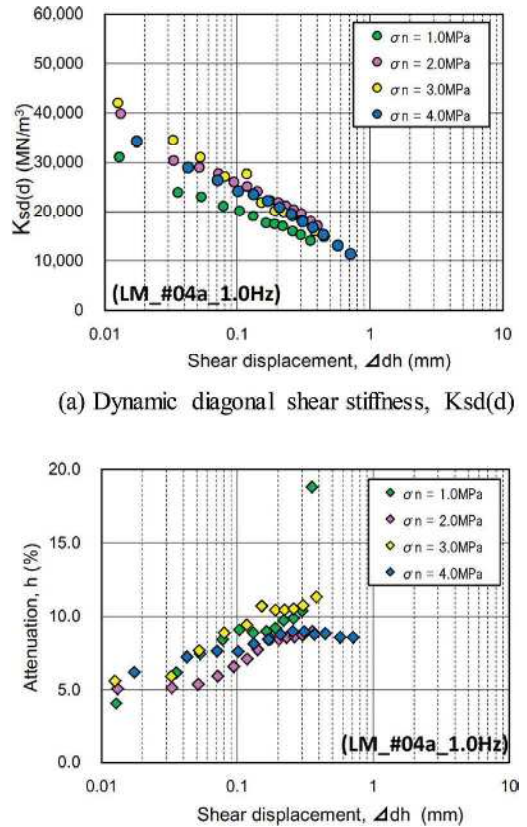


Figure 11. Dependence for the shear displacement amplitude of the dynamic shear parameter

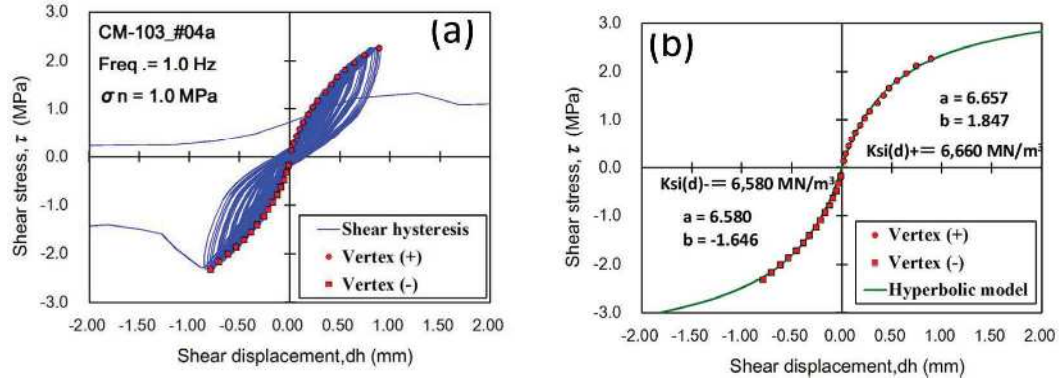


Figure 12. Shear hysteresis and vertex of skelton curve

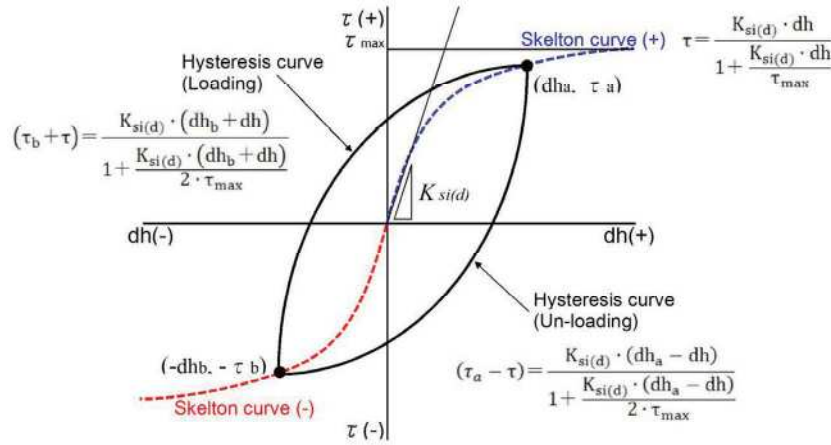


Figure 13. Hyperbola model

these points is called a frame curve (Skelton curve) generally.

Figure 12(b) shows the positive vertex and negative vertex, and was similar by a hyperbola model in each. The hyperbola model models the skelton curve indicating shear stress,  $\tau$  - shear displacement,  $dh$  relations by hyperbolic function.

Figure 13 shows hyperbola model for rock joints. In Figure 13, the skelton curve is modelled by a hyperbola model, and the history curve is displayed by Masing rule.

#### 4 CONCLUSION

In this study, we examined a dynamic strength and deformability of rock discontinuity, than a large number of dynamic direct shear test results for a rock discontinuities and mortar artificial discontinuities.

The authors defined dynamic peak shear strength  $\tau_p(d)$  and defined dynamic diagonal shear stiffness,  $K_{sd(d)}$  and attenuation,  $h$ . Also we examine the characteristic about these dynamic parameters and suggest the modeling by the hyperbola model.

#### REFERENCES

- Yoshida, J., Yoshinaka, R. & Sasaki, T. 2014. Study on Dynamic Properties of Rock Discontinuity using Dynamic Direct Shear Test Machine. ARMS8, 8th Asian Rock Mechanics Symposium, 14–16 October 2014, Sapporo Japan
- Iwata, N., Sasaki, T., Sasaki, K., Yoshinaka, R., 2012, Static and dynamic response analysis of rock mass considering joint distribution and its applicability, Proc. 12th ISRM Congress, 233–236.
- Yoshinaka, R., Iwata, N. and Sasaki, T., 2012, Applicability of Multiple Yield Model to earthquake response analysis for foundation rock of large-scale structure, Jour. of JSCE, 451–465.